Proceedings of ICRC 2001: 522 © Copernicus Gesellschaft 2001

ICRC 2001

EAS simulations at Auger energies with CORSIKA

M. Risse[1], **D. Heck**[1], **J. Knapp**[2], **and S. S. Ostapchenko**[1,*]

[1]Institut für Kernphysik, Forschungszentrum Karlsruhe, 76021 Karlsruhe, Germany
[2]Department of Physics and Astronomy, University of Leeds, Leeds LS2 9JT, U.K.
[*]On leave of absence from the Moscow State University, Moscow, Russia

Abstract. The air shower simulation program CORSIKA is used to study the cascades initiated by the highest-energy cosmic rays. Due to different detection techniques of current experiments, the shower simulation should provide all necessary information on the production of fluorescence and Cherenkov photons during the cascade development and on the particle component reaching observation level. Additionally, the amount of CPU time and disk space should allow for the production of a large number of events to investigate shower fluctuations and the dependence on primary parameters. With respect to these requirements, the present CORSIKA usage is summarized with special focus on the application of particle thinning. A basic method to treat weighted particles in the detector simulation is proposed. Extensions concerning the fluorescence and Cherenkov light description are discussed. First results on the distribution of the energy deposit of charged particles in air showers, which is closely connected to the fluorescence light production, are given.

1 Introduction

The Auger experiment (Auger Collaboration, 1997) begins the exploration of the highest-energy cosmic rays with a prototype installation. Parallel to first measurements, a large data base of simulated extensive air showers (EAS) is prepared using the CORSIKA code (Heck et al., 1998). Since the detailed simulation of all produced secondary particles (of the order of 10^{13} secondaries in a 10^{20} eV shower) is impossible, thinning techniques are applied. Generation and transport of individual fluorescence and Cherenkov photons is also prohibited by the huge number of photons, exceeding the particle number by more than 3 orders of magnitude. Thus, to allow for a realistic simulation of fluorescence and Cherenkov light CORSIKA is being extended to enable a detailed mapping of the longitudinal cascade development.

In the first part of the paper, the current philosophy and experiences for preparing a CORSIKA shower library are described. Especially, aspects concerning the technique of particle thinning are discussed. In the second part, the status and first results of extracting information on fluorescence and Cherenkov light production are presented.

Correspondence to: M. Risse (risse@ik1.fzk.de)

2 Shower generation

2.1 CORSIKA

CORSIKA is an open program package for performing a complete 4-dimensional simulation of air showers with primary energies from sub-TeV to $>10^{20}$ eV. For the treatment of particle interactions, external state-of-the-art codes are employed. Electromagnetic interactions are simulated using a tailer-made version of the EGS4 code (Nelson et al., 1985). Due to the large theoretical uncertainties in the description of hadronic interactions, different high-energy and low-energy hadronic interaction models are to the user's disposal. For a recent model comparison, see Heck et al. (2001).

The usage of CORSIKA in connection with experiments of completely different detection techniques and simulation requests (e.g., arrays measuring the electromagnetic, muonic, and hadronic component, Cherenkov and neutrino telescopes, μ^+/μ^--charge ratio measurements) guarantees continuous critical checks, improvements, and extensions both of the simulation code itself and, by comparing with measurements, of the physics implemented. For the simulation of the highest-energy cosmic rays, the LPM effect (Landau and Pomeranchuk, 1953; Migdal, 1956) and techniques of particle thinning (see chapter 2.2) have been implemented (Heck and Knapp, 1998). Three hadronic interaction models reach to the highest energies: QGSJET 01 (Kalmykov et al., 1997; for the recent modifications, see Heck et al., 2001), DPMJET II.5 (Ranft, 1999), and SIBYLL (Fletcher et al., 1994; Engel et al., 1999). Cherenkov light production is possible. The energy deposit of charged particles is calculated for the subsequent modeling of the fluorescence light production.

2.2 Particle thinning

To keep the CPU times and particle output files in reasonable limits, for the simulation of highest primary energies the *thin sampling* option is available in CORSIKA. When activated, this option does not treat in detail all secondary particles, it

samples "representative" particles which are followed further on and weighted accordingly, while the bulk of particles is discarded (Hillas, 1997). This thinning starts at a selectable fraction of the primary energy. The additional use of an optimum weight limitation for the particles leads to a much better simulation performance (Kobal et al., 1999) in terms of decreased additional ("artificial") fluctuations, introduced by thinning, and computing time. Especially, optimal thinning includes different weight limits for the electromagnetic component compared to the muonic and hadronic ones.

For illustration, let's suppose a primary energy of $E_0 = 10^{19}$ eV and an optimized thinning of 10^{-6}. Then, a detailed simulation is performed down to particle energies of 10^{13} eV. Below this energy the thinning algorithm is employed until a weight limit is reached of $E_0/\mathrm{GeV} \cdot 10^{-6} = 10^4$ for electromagnetic particles and of 10^2 for muons and hadrons. Below these energies, i.e. about 10^9 eV (e/γ) and 10^{11} eV (μ/had), again the detailed simulation starts until simulation threshold.[1] Using instead a thinning of 10^{-7} *without* weight limits, particles with weights up to 10^7 (e/γ) and 10^4 (μ/had) are produced. The latter method will suffer from much larger artificial fluctuations. Also when comparing the data output, it is evident that the typical file size of $\simeq$350 MB (per shower!) with optimized 10^{-6} thinning yields a much better shower representation compared to $\simeq$20 MB using 10^{-7} thinning only.[2] Thus, for achieving best performance in terms of good data quality and small computing time, the use of optimized thinning is of crucial importance.

However, special care must be paid to control and perhaps *a posteriori* decrease the influence of artificial fluctuations introduced by thinning. Also, it is not evident how to treat weighted particles in a detector simulation. The statistical uncertainty in, e.g., the particle number in a given area is

$$\sigma_N = \sqrt{\langle N^2\rangle - \langle N\rangle^2} = \sqrt{\langle \left(\sum_{i=1}^{n} w_i\right)^2 \rangle - \langle \sum_{i=1}^{n} w_i\rangle^2} \quad (1)$$

for n particles with individual weights w_i which represent $N = \sum_i w_i$ particles. Denoting the average particle weight for an individual event as $W = \frac{1}{n}\sum_i w_i$, from (1) we gain

$$\sigma_N = \sqrt{\langle n^2W^2\rangle - \langle nW\rangle^2} \ . \quad (2)$$

This formula takes a very simple and easily understandable form when considering the particle weights to be constant, $W = \mathrm{const}$, and assuming that the fluctuations of the number of "thinned" particles n obey Poisson statistics, i.e. $\sigma_n = \sqrt{\langle n^2\rangle - \langle n\rangle^2} = \sqrt{\langle n\rangle}$. Then from (2) we obtain

$$\sigma_N = W\sqrt{\langle n\rangle} = \sqrt{W\langle N\rangle} \ . \quad (3)$$

Thus, large weights result in huge artificial fluctuations exceeding by far the "natural" ones, which consist both of shower-to-shower and of physical Poissonian fluctuations.[3] The artificial fluctuations reduce to the physical Poissonian of the "real" particle number N, $\sigma_N \to \sqrt{\langle N\rangle}$, only in the limit $W \to 1$.

To *a posteriori* decrease the artificial fluctuations, particles are collected from an area A_{coll} much larger than the detector area A_{det} (typically of the order of 10 m^2). The weights then are rescaled according to the ratio of both areas, $w_i^{new} = w_i \cdot (A_{det}/A_{coll})$. Limitations of this method are given by the effect of smoothing over the collecting area which contains both lateral gradients of densities, time delays etc. (which, to some extent, can be accounted for), larger-scale granularities and correlations of particles coming from the same subshower. To keep the collecting area and such effects small, again the use of optimal thinning is important, since larger particle weights require a larger collecting area. The approach used in the current Auger surface detector simulation and corresponding limitations are described by Billoir (2000).

To avoid rescaled weights $w_i^{new} > 1$ and duplication of (perhaps "fractional") particles for a detector simulation, the following method might be appropriate. The collecting area is chosen to be

$$A_{coll} = w_{max} \cdot A_{det} \ \Rightarrow w_i^{new} \leq 1 \quad \text{for all particles.} \quad (4)$$

Now, the interpretation of the weights $w_i^{new} \leq 1$ is the probability of the particle to be considered in the detector simulation. Optimal thinning with limited w_{max} could assure that A_{coll} is reasonably small. In the aforementioned case of optimal 10^{-6} thinning with $E_0 = 10^{19}$ eV, a collecting area of $10^4 \cdot A_{det}$ would be sufficient for e/γ, for μ/had even only $10^2 \cdot A_{det}$. Without optimal thinning the collecting areas typically are considerably larger even when particles with weights $w_i^{new} > 1$ are allowed (Billoir, 2000).

2.3 Shower Library

For the interpretation of the Auger data, a shower library is prepared at the computing center of IN2P3 in Lyon (France).[4] The typical production rate is 80−100 GB/week using simultaneously $\simeq$30 Linux 750 MHz Pentium Processors. This corresponds to roughly 2000 (200) highest-energy showers of optimized 10^{-5} (10^{-6}) thinning per week. The files are stored in a mass storage. Some shower information like the longitudinal energy deposit, are kept in small size files on local disk to allow conveniently some analyses.

Apart from simulation runs with specific parameter requirements, the current simulation strategy is twofold: Firstly, showers of (different) fixed primary energy and zenith angle are calculated with very good thinning quality of optimized 10^{-6} thinning. The energy - zenith angle combinations are chosen to cover in particular the parameter ranges important for the Auger Engineering Array. These showers, for instance, might be used to obtain shower parametrizations. Secondly, a non-discrete primary parameter distribution is chosen. The primary energies follow a power law (differential index of -2.0) with zenith angles out to 60°. To achieve

[1] Usually 100 keV for e/γ and 100 MeV for μ/had.

[2] CPU times are only doubled for optimized 10^{-6} thinning.

[3] Natural and artificial fluctuations in the Auger surface detector are discussed in detail by Billoir (2001).

[4] See http://webcc.in2p3.fr/ for more information on CC-IN2P3.

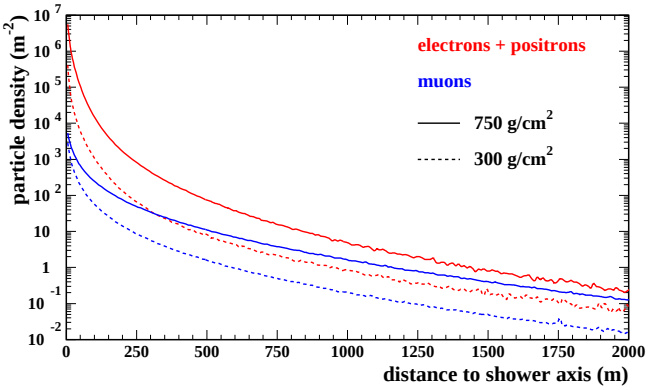

Fig. 1. Particle densities of $e^{\pm}$ and $\mu^{\pm}$ for proton primaries of $E_0 = 10^{19}$ eV at two different atmospheric levels.

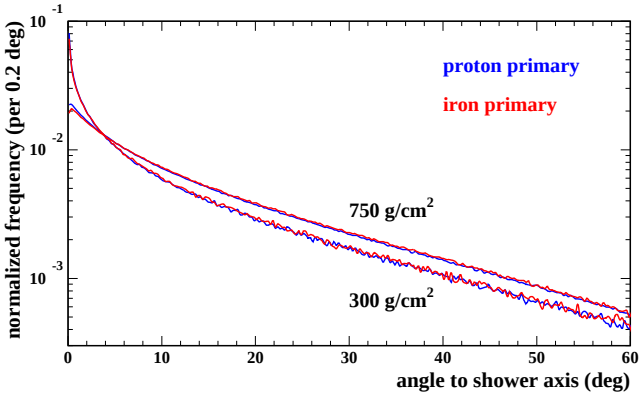

Fig. 2. Angular distribution (area normalized to one) of $e^{\pm}$ for proton and iron primaries of $E_0 = 10^{19}$ eV at two different atmospheric levels.

high statistics for these showers an optimized 10^{-5} thinning is used. For both strategies different primary particles as protons, iron nuclei, photons, etc. are simulated and the statistics is permanently increased.

As hadronic interaction model, QGSJET 01 is employed because analyses, though at smaller primary energies, have shown that this model provides the best overall description of EAS data (see, e.g., Antoni et al., 1999).

3 Fluorescence and Cherenkov light treatment

Two problems arise when treating fluorescence and Cherenkov light, observable by optical telescopes, in an air shower simulation: Firstly, a realistic transport description has to take atmospheric conditions as ozone or aerosol concentrations into account which vary with time. Thus, to allow a reuse of a (time-intensive!) air shower simulation, informations on the light production are given. The atmospheric transport is subject to a separate program. Secondly, the number of optical photons exceeds by orders of magnitudes the particle number and prohibits an individual consideration. A method to account for this is the extraction of detailed information for a limited number of levels of the cascade development (*longitudinal mapping*).

In the following, for vertical showers of $E_0 = 10^{19}$ eV, particle distributions are compared at atmospheric depths of 300 g/cm^2 and 750 g/cm^2 (close to shower maximum).[5] Insights into the light production can already be gained by investigating the emitting particles (chapter 3.1). More directly, the energy deposit of charged particles (for fluorescence, chapter 3.2) and the Cherenkov routines available in CORSIKA can be used (chapter 3.3). Apart from the possibility to study the shower physics of highest-energetic cascades in general, the technique of longitudinal mapping might help to look for suitable parametrizations and/or provide information in each single shower for a realistic fluorescence and Cherenkov light treatment.

[5] Optimal 10^{-6} thinning, average of 8 proton and 4 iron induced showers, respectively.

3.1 Emitting particles

In figure 1, particle lateral distributions are displayed. The particle number increase with X (atmospheric depth) can be seen. As expected, the muon lateral distribution is flat compared to that of $e^{\pm}$. The shape especially of the $e^{\pm}$ lateral distribution depends only weakly on X which is related to the smaller amount of matter per unit length at small X. The angular distributions of $e^{\pm}$ are given in figure 2. With increasing X, larger angles are more frequently. About 13.2 % (17.1 %) of the particles have angles $> 30^{\circ}$ at 300 g/cm^2 (750 g/cm^2). The distributions for iron and proton primaries resemble each other. Finally, from the energy spectra shown in figure 3, the reduction of the average energy of $e^{\pm}$ and of the number of high-energy $e^{\pm}$ with increasing depth is visible. For iron primaries, the earlier development leads to a higher particle number at 300 g/cm^2, and the smaller energy per primary nucleon results in less high-energetic $e^{\pm}$.

3.2 Fluorescence light

The production of fluorescence photons is closely connected to the energy deposit of charged particles in air (Kakimoto et al., 1996). CORSIKA tabulates the energy deposit of the different particle components as a function of X, usually in layers of thickness 5 g/cm^2 (adjustable). In this approximation of a shower as a 1-dimensional line, the subsequent calculation of the fluorescence production is possible, taking into account temperature and pressure dependences etc. of the fluorescence yield (Kakimoto et al., 1996). To study the real size and the time-dependent signal of a shower as seen in the fluorescence light, figure 4 shows the development of the lateral energy deposit generated by $e^{\pm}$. Similar to the results of figure 1, the shapes do not depend significantly on the depth. While at smaller X, due to the earlier development, the energy deposits from iron primaries exceed on average those from protons, they resemble each other at larger depths for

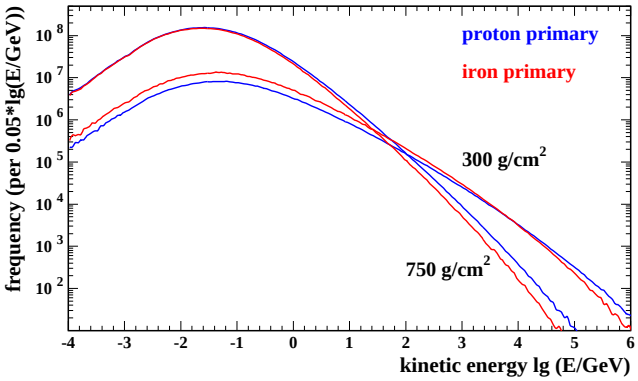

Fig. 3. Kinetic energy spectra of $e^{\pm}$ for proton and iron primaries of $E_0 = 10^{19}$ eV at two different atmospheric levels.

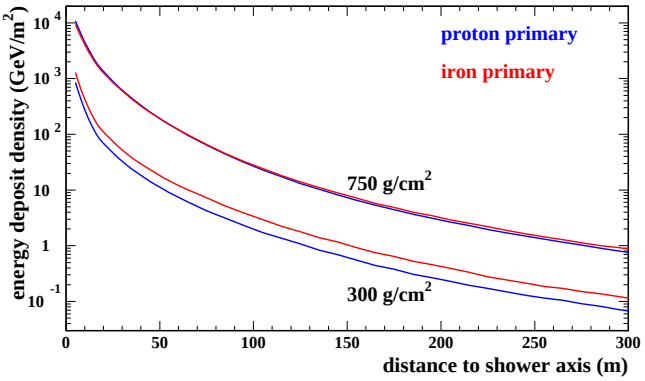

Fig. 4. Energy deposit density of $e^{\pm}$ vs. distance to shower axis, for proton and iron of $E_0 = 10^{19}$ eV at two different atmospheric levels.

distances out to a few 100 m.

3.3 Cherenkov light

With enabled Cherenkov option, CORSIKA calculates the number and emission direction of the Cherenkov photons in the chosen wavelength interval produced by the individual particles (which might have weights). The photons can be grouped to bunches of adjustable size (analogous to particle weights) with a common emission direction for the bunch. The idea currently followed is to activate the Cherenkov routines in CORSIKA for several small atmospheric layers (thickness of the order 1 g/cm^2). In these layers, correlated properties of the produced Cherenkov light are extracted, e.g. emission angles as a function of distance to shower axis.

4 Summary and outlook

The features of CORSIKA with respect to the simulation of the highest primary energies, and first experiences in preparing a mass production have been discussed. Special attention was paid to the question of particle thinning. Using weight limitation in terms of optimal thinning leads *a priori* to reduced artificial fluctuations. *A posteriori*, it is expected to allow a better reduction of artificial fluctuations and an elegant method to treat particle weights in a detector simulation. In this method, the rescaled weights are ≤ 1 and are interpreted as accepting probabilities. Further and more quantitative investigations are needed.

Currently, CORSIKA is extended to allow a detailed mapping of the longitudinal shower development. In particular, this aims to provide the necessary informations on fluorescence and Cherenkov light production. Thus, subsequently a realistic propagation of the light through the atmosphere and a detector simulation can be carried out.

Acknowledgements. We are indebted to W. Wojcik and colleagues of the IN2P3 and to J.N. Albert, A. Cordier, and E. Cormier for their continuous help and patient advice when preparing the mass production, and to many Auger Collaboration members for fruitful discussions. The partial support of this work by the British German Academic Research Collaboration from The British Council and the DAAD is acknowledged.

References

Antoni, T., et al., KASCADE Collaboration, *J. Phys. G: Nucl. Part. Phys.* **25**, 2161, 1999.
Auger Collaboration, *The Pierre Auger Observatory Design Report* (1997), http://www.auger.org/admin/DesignReport/index.html
Billoir, P., *Auger GAP note* 2000-025, 2000.
Billoir, P., *Auger GAP note* 2001-005, 2001.
Engel, R. et al., *Proc.* 26^{th} *Int. Cosmic Ray Conf.*, Salt Lake City (USA), **1**, 415, 1999.
Fletcher, R.S. et al., *Phys. Rev.* **D50**, 5710, 1994.
Heck, D. et al., Report **FZKA 6019**, Forschungszentrum Karlsruhe, 1998; see http://www-ik3.fzk.de/∼heck/corsika .
Heck, D., and Knapp, J., Report **FZKA 6097**, Forschungszentrum Karlsruhe, 1998.
Heck, D. et al., *Proc.* 27^{th} *Int. Cosmic Ray Conf.*, Hamburg (Germany), Contribution HE 1.3.1, 2001.
Hillas, A.M., *Nucl. Phys. B (Proc. Suppl.)* **52B**, 29, 1997.
Kakimoto, F., et al., *Nucl. Instr. Meth.* **A 372**, 527, 1996.
Kalmykov, N., Ostapchenko, S., and Pavlov, A.I., *Nucl. Phys. B (Proc. Suppl.)* **52B**, 17, 1997.
Kobal, M., Filipčič, A., and Zavrtanik, D. for the Pierre Auger Collaboration, *Proc.* 26^{th} *Int. Cosmic Ray Conf.*, Salt Lake City (USA), **1**, 490, 1999.
Landau, L.D., and Pomeranchuk, I.Ya., *Dokl. Akad. Nauk SSSR* **92** 535 & 735, 1953.
Migdal A.B., *Phys. Rev.* **103** 1811, 1956.
Nelson, W.R., Hirayama, H. and Rogers, D.W.O., Report **SLAC 265**, Stanford Linear Accelerator Center, 1985.
Ranft, J., preprints hep-ph/9911213 and hep-ph/9911232, 1999.